ACS APPLIED MATERIALS & INTERFACES

Research Article

www.acsami.org

Reorganization of Cytoskeleton and Transient Activation of Ca^{2+} Channels in Mesenchymal Stem Cells Cultured on Silicon Nanowire Arrays

Dandan Liu,[†,‡] Changqing Yi,[†,‡,∥] Kaiqun Wang,[§] Chi-Chun Fong,[†,‡] Zuankai Wang,[§] Pik Kwan Lo,[‡] Dong Sun,[§] and Mengsu Yang*[,†,‡]

[†]Key Laboratory of Biochip Technology, Biotech and Health Centre, Shenzhen Research Institute of City University of Hong Kong, Shenzhen, China

[‡]Department of Biology and Chemistry and [§]Department of Mechanical and Biomedical Engineering, City University of Hong Kong, Hong Kong, China

[∥]Key Laboratory of Sensing Technology and Biomedical Instruments (Guangdong Province), School of Engineering, Sun Yat-Sen University, Guangzhou, China

ABSTRACT: Tissue engineering combines biological cells and synthetic materials containing chemical signaling molecules to form scaffolds for tissue regeneration. Mesenchymal stem cells (MSCs) provide an attractive source for tissue engineering due to their versatility of multipotent differentiation. Recently, it has been recognized that both chemical and mechanical stimulations are essential mediators of adhesion and differentiation of MSCs. While significant progress has been made on the understanding of chemical regulatory factors within the extracellular matrix, the effects of mechanical stimulation exerted by nanomaterials on MSCs and the underlying mechanisms are less well-known. The present study showed that the adhesion, proliferation, and differentiation of MSCs cultured on vertically aligned silicon nanowire (SiNW) arrays were significantly different from those on flat silicon wafer and control substrates. The interactions between MSCs and the SiNW arrays caused the stem cells to preferentially differentiate toward osteocytes and chondrocytes but not adipocytes in the absence of supplementary growth factors. Our study demonstrated that Ca^{2+} ion channels were transiently activated in MSCs upon mechanical stimulation, which eventually led to activation of Ras/Raf/MEK/ERK signaling cascades to regulate adhesion, proliferation, and differentiation of MSCs. The stretch-mediated transient Ca^{2+} ion channel activation and cytoskeleton reorganization during stem cell−nanowire interaction may be early events of lineage-specific potentiation of MSCs in determining the fates of mesenchymal stem cells cultured on microenvironments with specific mechanical properties.

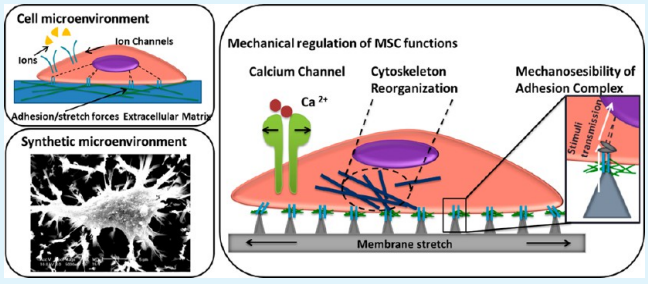

KEYWORDS: *silicon nanowire array, mesenchymal stem cell, differentiation, mechanical stimulation, Ca^{2+} ion channels*

1. INTRODUCTION

Nanomaterial-based scaffolds have shown great promise for a wide range of clinical applications as biocompatible materials.[1−3] Bone marrow derived mesenchymal stem cells (MSCs) can differentiate into multiple cell types including osteoblasts, chondrocytes, adipocytes, and other tissues of mesenchymal origin and have been incorporated with various materials to develop scaffolds for regeneration of tissues including bone, cartilage, ligament, skeletal muscle, and tendon.[4,5] Therefore, it is important to understand the interactions between MSCs and nanomaterials at cellular and molecular levels to better design biocompatible nanomaterials for tissue engineering.

The renewal and differentiation of MSCs are regulated by extracellular environments such as chemical and mechanical stimuli. Numerous studies in the field of biomaterials have demonstrated that surface chemistry of the cellular environment is an essential parameter contributing to the functions of MSCs.[6] Similarly, the mechanical properties of the cell culture environment have also been shown to stimulate and regulate the functions of MSCs.[7,8] While significant progress has been made on the understanding of chemical regulatory factors within the extracellular matrix, the effects of mechanical stimulation exerted by nanomaterials on MSCs and the mechanisms underlying such effects are less well-known.

In this study, vertically aligned silicon nanowire (SiNW) arrays were prepared and used as substrates to culture MSCs, and the effects of SiNWs on the behaviors MSCs were investigated. SiNW arrays were chosen because of their biocompatibility, noncytotoxicity, and biodegradability.[9,10] The adhesion, proliferation, cytoskeleton remodeling, and

Received: September 29, 2013
Accepted: December 5, 2013
Published: December 5, 2013

differentiation of MSCs were studied at the cell/nanomaterial interface in the absence of specific supplementary factors for stem cell differentiation. It has been reported that the mechanical properties of cells measured by different techniques such as atomic force microscopy (AFM), micropipet aspiration, and magnetic twisting cytometry would change when cultured on different substrates.[11−14] We used scanning electron microscope (SEM) and immunofluorescence staining techniques to study the adhesion and morphology of MSCs and the cytoskeleton structures of MSCs cultured on SiNW arrays. Laser tweezer technique was used to measure the mechanical properties of adherent MSCs cultured on SiNW arrays, where the deformation of the cell under optically induced stretching was determined at single cell level. Because cell adhesion and spreading are associated with cytoskeletal tension, changes in cell morphology and cytoskeletal structure are very important in regulating MSC viability and differentiation.[15] The differentiation of MSCs toward osteocytes, chondrocytes, and adipocytes was studied for MSCs cultured on SiNWs in the absence of differentiate-inducing factors. We also demonstrated that the increasing spreading and cytoskeleton-driven tension of MSCs induced by SiNWs was associated with osteogenic and chondrogenic differentiation but not adipogenic differentiation of MSCs. We further hypothesized that SiNW arrays acted on mechanosensors located on the cell membrane which transduced mechanosensitive signals into the nucleus via bridging and signaling proteins. The activation of Ca^{2+} ion channels of MSCs upon interacting with SiNWs was measured as a function of time. The expression of several key genes associated with Ca^{2+} ion channel activation and involved in the MAPL/ERK signaling pathway was also determined to understand how the SiNWs in the culturing microenvironment affect MSC differentiation.

2. EXPERIMENTAL SECTION

2.1. Fabrication of Silicon Nanowire Array (SiNW Array). The fabrication process of vertically aligned SiNW arrays was performed according to the method described in Zhang et al.[16] Briefly, the silicon wafer was degreased by ultrasonication in acetone and ethanol for 30 min each. Then, the degreased silicon wafer was immersed in H_2SO_4/H_2O_2 solution and HF solution for 1 h each. For the etching process, a thick Ag nanoparticle film was deposited on the silicon wafer as a catalyst. Subsequently, the etching process was carried out in a solution of HF/H_2O_2 at 60 °C. Different length and density of nanowires could be obtained by controlling the etching duration and the concentration of HF/$AgNO_3$ solution. After etching, the silicon wafer was immersed in the solution of HCl/HNO_3 to remove the Ag film. The silicon nanowire array was characterized by a scanning electronic microscope (Philips XL 30).

2.2. Isolation and Characterization of MSCs. Four to six weeks Kunming female mice were used to isolate MSCs from bone marrow (Medical Laboratory Animal Center of Guangdong Province) as previously described.[17] The mice were killed by cervical dislocation. Femora and tibiae were cleaned to remove the adherent tissue, and the bone marrow was harvested by flushing out with Dulbecco's Modified Eagle Medium (DMEM) supplemented with 10% fetal bovine serum (FBS) and the antibiotic (100 U/mL of penicillin and 100 g/mL of streptomycin (BBI, Canada)). After 3 days, nonadherent cells were removed by washing with PBS, and the adherent cells were collected by trypsinization. The medium was changed every 3 days. The MSCs were characterized by positive markers (CD44 and Oct4), together with the negative marker CD14 through immunofluorescent staining and multiparameter flow cytometry.

2.3. Immunofluorescence Staining for Phenotypic Analysis. For immunophenotyping, MSCs were detached and washed once with 0.5% BSA in PBS and incubated with the following primary antibodies, CD44-PE, CD14-FITC, and Oct4-Alexa Fluor 488, at room temperature for 30 min. The cells were then washed and resuspended in 1% BSA/PBS for analysis on a flow cytometer (BD FACS Canto II, USA). Cells without immunostaining were used as negative control.

For the immunofluorescent staining, MSCs were fixed with 4% paraformaldehyde in PBS for 30 min and then permeabilized with 0.2% Triton X-100/PBS (PBSTX) for 30 min. Thereafter, cells were incubated with fluorescent antibodies in PBS for 30 min at room temperature followed by washing and mounting on glass slides. For the osteogenesis and chondrogenesis phenotypic analysis, differentiated MSCs were incubated with osteogenic (ALP-Cy3) and chondrogenic specific (CD151-Cy5) antibodies, respectively. Finally, the cell nuclei were stained with DAPI (Sigma-Aldrich). The slides were scrutinized field by field with a confocal microscope (Leica TCS-SPE, Germany).

2.4. Adherent Ability and Morphology of MSCs. MSCs were seeded on SiNW arrays (1 cm × 1 cm) and a flat Si wafer in a 48-well plate at the density of 1×10^4/well. After 24 h of cell seeding, nonadherent cells were removed by washing three times with PBS. The adherent cells were collected by trypsinization, and trypan blue was added for 5 min. The number of cells was counted in a hemocytometer. The adherent ability was expressed as the average number of live cells on a SiNW array or flat Si wafer compared to that on a Petri dish. Meanwhile, the viability of adherent cells was quantified by MTT assay.[17]

Morphological study of MSCs was performed by SEM after 4 days of cell culture. The cells were fixed with 2% glutaraldehyde buffer for 1 h and post fixed for 1 h in 1% osmium tetroxide. Subsequently, the SiNW array and wafer were dehydrated in gradient ethanol for 10 min each. The specimens were dried with hexamethyldisilazane (HMDS) followed by gold deposition and imaged under SEM to observe the morphology of MSCs.

2.5. Measurement of Cell Deformation Using an Optical Tweezer. The deformation of MSCs was measured with an optical tweezer system (BioRyx200; Arryx), which consists of a continuous wave laser beam with a wavelength of 1064 nm, an inverted microscope (Nikon TE2000, Japan), a holographic optical trapping device, a motorized stage (ProSan, Prior Scientific), and a charge-coupled device camera (FO124SC, Foculus). Experimental procedures and theoretical modeling were based on work by Tan et al.[18,19] Briefly, cells with two microbeads attached to diametrically opposite ends were selected for the experiment. A continuous wave laser beam was adopted to create multiple optical traps. One bead was held by one trap, while the other was moved by dragging another trap. Increasing membrane tension was applied to the cell by progressively extending the distance between the beads. The cell was stretched until one of the beads escaped the trap. After the bead was released, the cell gradually restored to its original shape. Then the elongation of cells along the direction of the optical axis was calculated and expressed by the image processing technique.[19,20] All the experiments were performed in a chamber, where the temperature and CO_2 concentration were set at 37 °C and 5%, respectively.

2.6. Alkaline Phosphatase Activity (ALP) Stain Assay. Th expression of ALP was evaluated to characterize the osteogenic differentiation of MSCs after 7 days of incubation on SiNW arrays. The cells were washed twice with ice-cold D-Hank's and fixed in 4% formaldehyde, then washed with distilled water, followed by incubation with ALP staining solution (Sigam, USA) for 30 min at 37 °C.

2.7. Mineralized Matrix Formation Assay. Alizarin Red staining assay was used to investigate the mineralization potential of MSCs incubated on the SiNW array. MSCs were grown on a SiNW array and wafer in 6-well plates for 18 days at the density of 5×10^5 cells per well. The cells were then rinsed with D-Hank's buffer, fixed with 95% ethanol at room temperature for 10 min, followed by incubation with 2% Alizarin Red S solution. The cells were then washed three times with D-Hank's, followed by rinsing three times with distilled water.

2.8. Chondrocyte Pellet Culture and Alcian-Blue Stain Assay. MSCs cultured on the SiNW array and wafer were detached and centrifuged at 1500 rmp for 5 min in 15 mL polypropylene conical

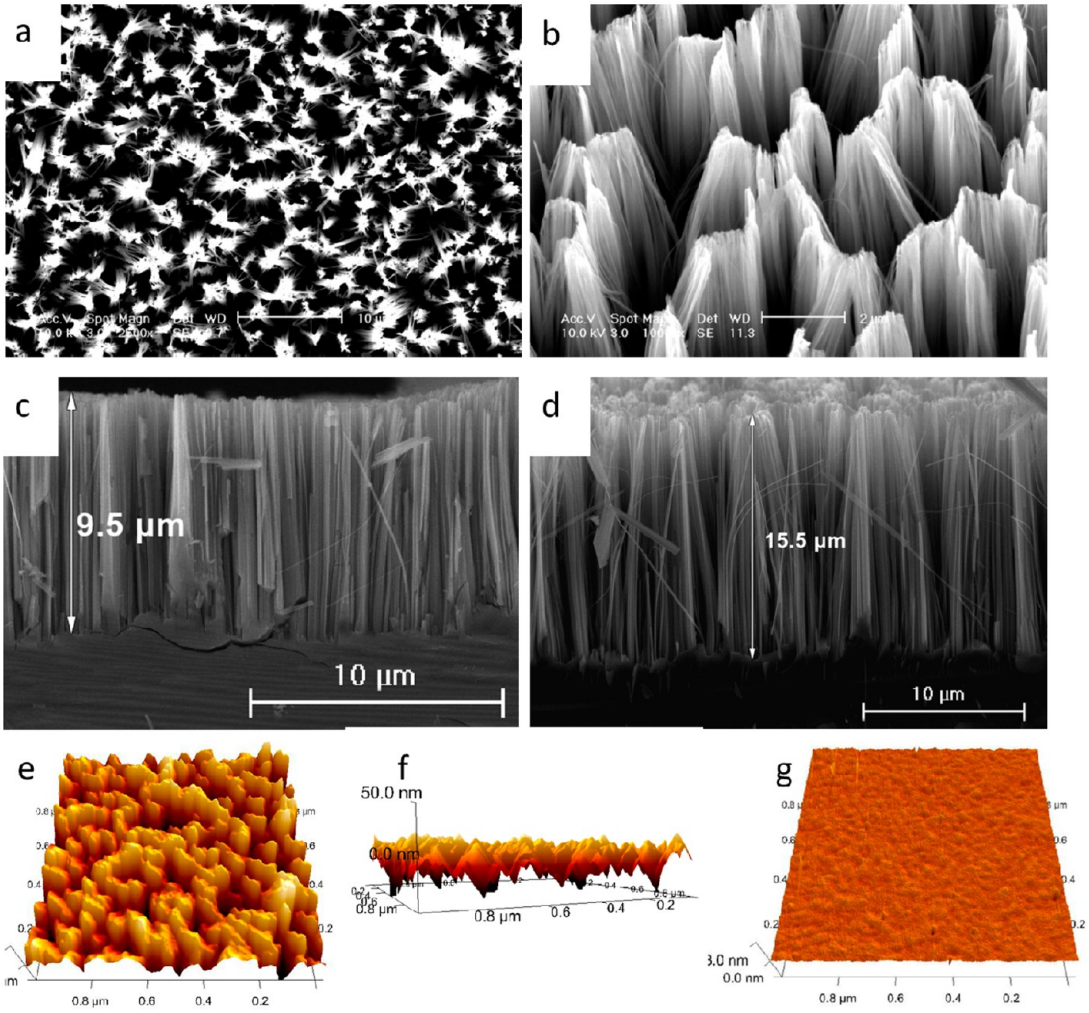

Figure 1. (a) Top view SEM images of SiNW. (b) Enlarged SEM image of SiNW array, tilt angle = 20°. (c and d) Side view SEM images of SiNW arrays. AFM phase images of SiNW array (e and f) and flat wafer (g).

tubes. The pellets were incubated for 21 days at 37 °C in an atmosphere containing 5% CO_2. At the end of the culture, the pellets were fixed with 4% formaldehyde in D-Hank's buffer for 15 min and embedded in paraffin, followed by staining with alcian blue.

2.9. Oil Red O Stain Assay. After 14 days of incubation on a SiNW array or flat wafer, MSCs were washed twice with D-Hank's and fixed with 4% formaldehyde for 30 min at room temperature. Fat droplets were stained by 0.6% (w/v) Oil red O solution (60% isoprapanol, 40% water) for 15 min at room temperature. Cells were then washed with distilled water to reduce the background dye for imaging.

2.10. Measurement of Cytosolic Calcium ($[Ca^{2+}]_i$). $[Ca^{2+}]_i$ was measured in a single cell using the fluorescent calcium indicator Fluo-3/AM. The mouse MSCs were isolated as above. After 4, 24, and 48 h preculturing on SiNW arrays, cells were incubated for 1 h in a Ca^{2+}-free Hank's balanced salt solution (HBSS) medium containing 6 μM/L Fluo3-AM. Then, the cells were washed three times with Ca^{2+}-free HBSS. Change of the intracellular calcium ion concentration $[Ca^{2+}]_i$ was determined by measuring the fluorescent intensity F under a confocal laser scanning microscope (Leica TCS SPE, Germany) at a scanning rate of 10 s with Ca^{2+}-free condition, based on the equation $[Ca^{2+}]_i = (F - F_0)/F_0$ (F_0 is the baseline value).

2.11. Quantitative Real-Time RT-PCR Analysis of Differentiation-Related Genes. The RT^{2}Profiler polymerase chain reaction (PCR) array (SABiosciences, USA) was used to evaluate the expression of differentiation-related genes in MSCs cultured on SiNW arrays for 4 days. Amplification by PCR was performed in a 25 μL reaction system according to the manufacturer's protocol from a SYBR Green Kit (SABiosciences, USA). The mRNA expression levels were normalized to glyceraldehyde phosphate dehydrogenase (GAPDH) and calculated by the $2^{-\Delta\Delta C_t}$ method. The $2^{-\Delta\Delta C_t}$ method is a widely used method to present relative gene expression, based on the data of the gene of interest (GOI) relative to a housekeeping gene (HKG). Due to the inverse proportional relationship between the threshold cycle (C_t) and the original gene expression level and the doubling of the amount of product with every cycle, the original expression level (L) for each GOI is expressed as: $L = 2^{-\Delta C_t}$. To normalize the expression level of a GOI to a HKG, the expression levels of the two genes are divided: $2^{-C_t(\mathrm{GOI})}/2^{-C_t(\mathrm{HKG})} = 2^{-[C_t(\mathrm{GOI})-C_t(\mathrm{HKG})]} = 2^{-\Delta C_t}$. To determine fold change in gene expression, the normalized expression of the GOI in the experimental sample (expt.) is divided by the normalized expression of the same GOI in the control sample (control): $2^{-\Delta C_t(\mathrm{expt})}/2^{-\Delta C_t(\mathrm{control})} = 2^{-\Delta\Delta C_t}$.

2.12. Statistical Analysis. Data are expressed as mean ± standard deviation. Statistical significance was done by using either the student t test for paired comparisons or the one-way ANOVA for multiple comparisons, and the value $P < 0.05$ was considered significant.

3. RESULTS AND DISCUSSION

3.1. Fabrication of the Silicon Nanowire Array (SiNW Array). Vertically aligned SiNW arrays were prepared on the surface of the Si wafer, where Figure 1a clearly showed that evenly distributed silicon nanowire arrays were vertically aligned on the Si wafer with different diameters and flower-

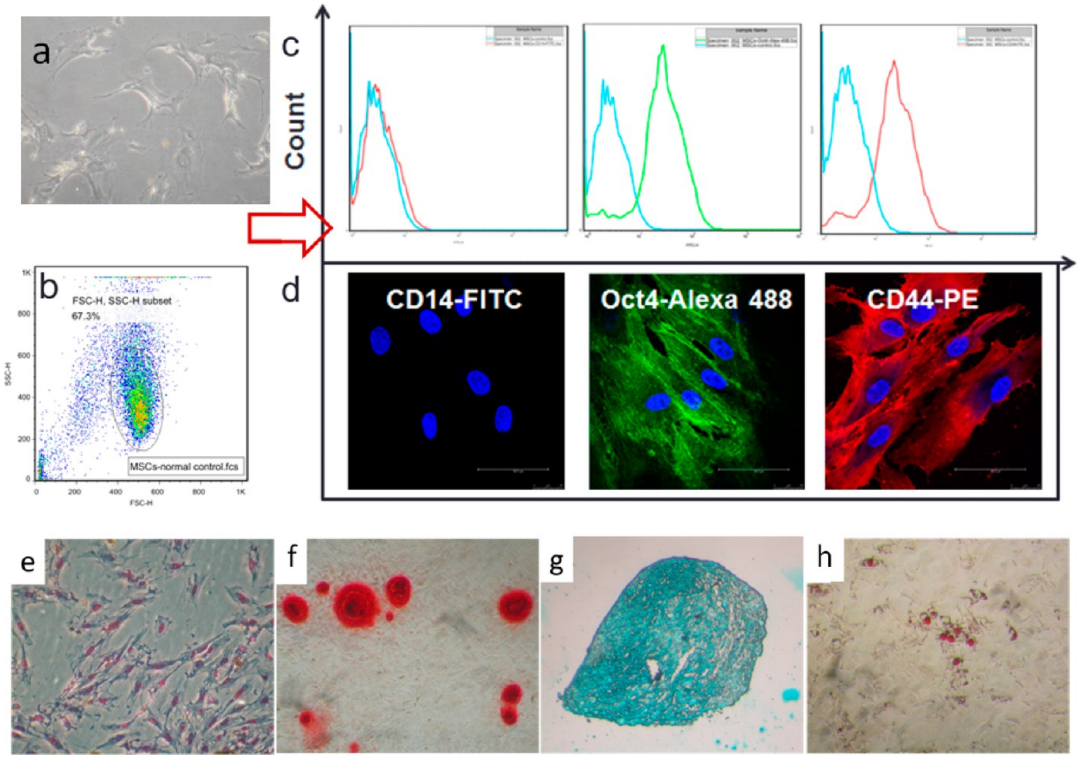

Figure 2. (a) MSCs with fibroblastic morphology. (b) Single cells were gated on FSC and SSC. (c) Stemness molecule characterization of the MSCs analyzed by flow cytometry after incubation with fluorescent dye-conjugated antibodies (anti-CD14, anti-Oct4, and anti-CD44). (d) Immunofluorescence images of stemness protein expression. Oct4 is represented by green fluorescence, while red and blue fluorescence indicates plasma membrane stained by anti-CD44 Ab and nucleus, respectively. (e) Osteogenic differentiation of MSCs stained by ALP. (f) Mineralized nodule formation stained by alizarin red S. (g) Chondrocytes stained by alcian blue. (h) Adipogenic differentiation of MSCs stained by oil red O.

like morphology (Figure 1b). As shown in Figure 1c and d, the length of SiNW arrays could be varied by controlling the duration of the etching process. The cross-sectional SEM images of SiNW arrays showed that the lengths of SiNWs were about 9.5 ± 1.5 μm and 15.5 ± 0.6 μm, for etching time of 30 min and 1 h, respectively. In contrast to a flat wafer (Figure 1g), atomic force microscopic images showed a uniform surface topology with silicon nanowires regularly arranged on the surface (Figure 1e and f).

3.2. Characterization of MSCs. The MSCs were isolated from mouse bone marrow and showed fibroblastic morphology (Figure 2a). CD44 and Oct4 are important stemness markers that have been shown to express in MSCs.[21−23] The positive markers (CD44 and Oct4) and the negative marker CD14 were used to confirm the identification of mouse MSCs by flow cytometry and a confocal microscope (Figure 2b−d). Specific assays for the identification of osteoblasts, chondrocytes, and adipocytes were performed to characterize the differentiation ability of the isolated mouse MSCs. As shown in Figure 2e and f, early stage osteogenic differentiation and late stage mineralized nodules formation were detected by the ALP staining and alizarin red S staining assay, respectively. The chondrocyte pellet was stained with alcian blue (Figure 2g) to show chondrogenic differentiation, while the adipocytes with lipid droplets were stained with oil red O for adipogenic differentiation (Figure 2h). The assay results confirmed that the MSCs readily differentiated into all three lineages under appropriate conditions.

3.3. Effects of SiNW Arrays on the Adherent Ability and Morphology of MSCs. The extracellular microenvironment is essential for modulating cell viability and providing niches to influence single and collective cell behaviors.[24] Cellular responses to mechanical stimuli are diverse, including cell-matrix adhesion, differentiation, and migration.[25] We observed that the MSCs adhered on the surface of the SiNW array (Figure 3a) better than on the flat Si wafer (Figure 3b). On average, the number of adherent cells cultured on SiNW arrays for 24 h was more than 3 times greater than that on the wafer (Figure 3d), and was approximately the same as the control (on petri dish). Since the MSCs were seeded at equal cell density on the two different substrates, the increase in the number of adherent MSCs on the SiNW array suggested the positive impact of the nanotopography on MSC survival and proliferation.

It has been suggested that MSCs could survive on silicon nanowires for several days.[26] We quantified the viability of the MSCs in the adherent population after 4 days of cell culture. As shown in Figure 3e, the viability of the attached cells on the SiNW array was similar to that on the control and yet significantly greater than that on the flat Si wafer, indicating that topological cues at the nanoscale were favorable for the survival and proliferation of MSCs.

Besides the adherent ability and viability, cell morphology also reflects the function and behavior of MSCs. SEM images showed a high degree of protrusions at the cell edge (Figure 3f) for the MSCs cultured on SiNW arrays. In addition to the conformal contact between MSCs and the SiNW array, these protrusions provided a strong adhesion force to the surface of the substrate. Through protrusions and cell−nanowire contacts, the MSCs were stretched on the nanowires, which appeared to bend toward the cell body (Figure 3g, red arrows). The SEM images clearly showed that the filopodia extensions were

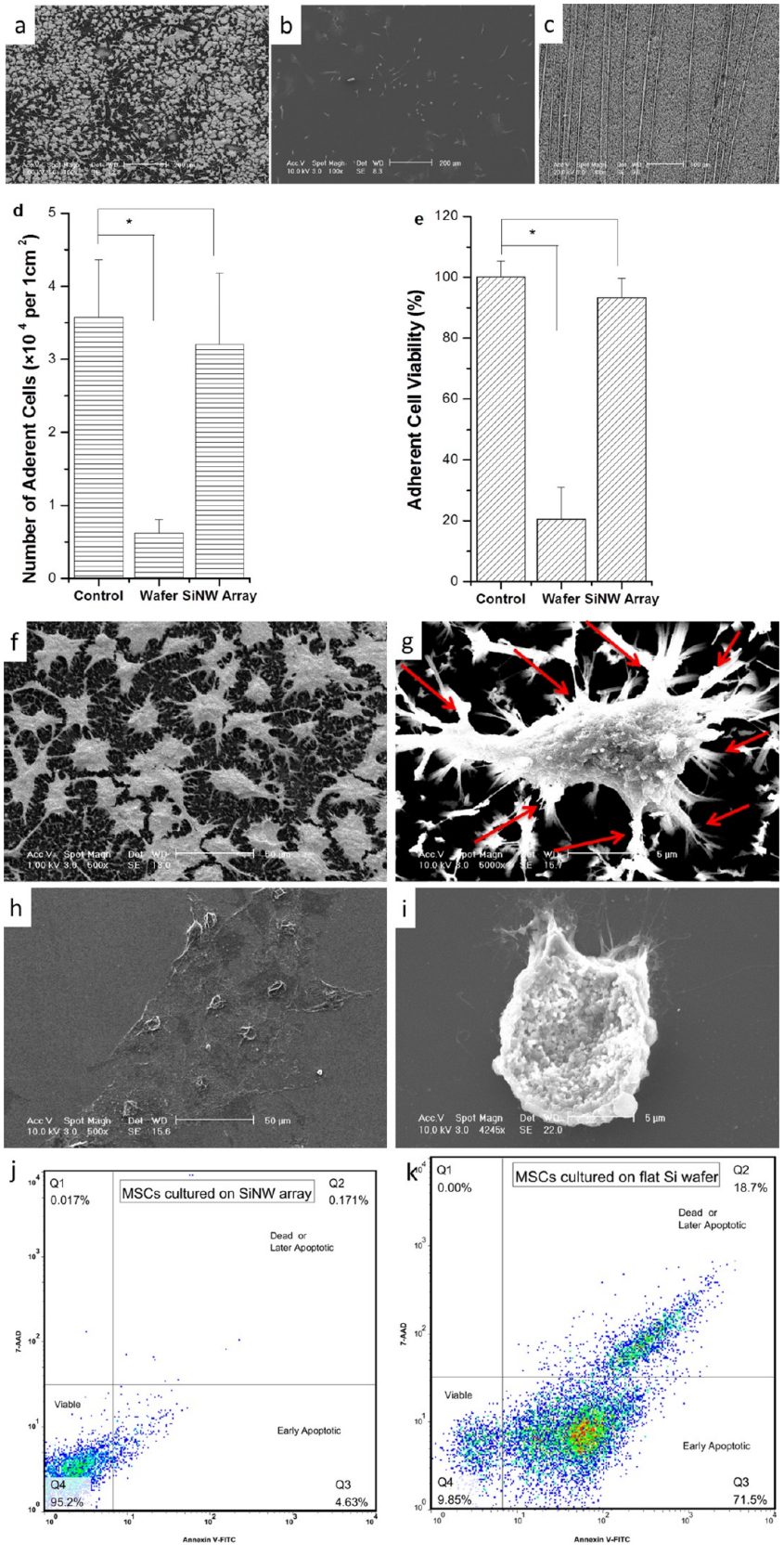

Figure 3. SEM images showing the morphology of MSCs on the (a) SiNW array and (b) flat Si wafer after 4 days of culture. (c) SME images showing no remaining cells on the SiNW array after detaching. (d) Adherence ability of MSCs on the SiNW array and wafer after 24 h of culture. (e) Adherent cell viability on SiNW array and wafer after 4 days of culture. Enlarged SEM morphology of cells grown on the SiNW arrays (f and g, the arrowhead points to a filopod) and on the flat Si wafer (h and i). Apoptosis was evaluated by Annexin-V staining after culturing MSCs on the SiNW array (j) and flat Si wafer (k), where flow cytometry images present Annexin-V-FITC staining in *x* axis and 7-AAD in *y* axis. (*$P < 0.05$, vs wafer, $n = 5$).

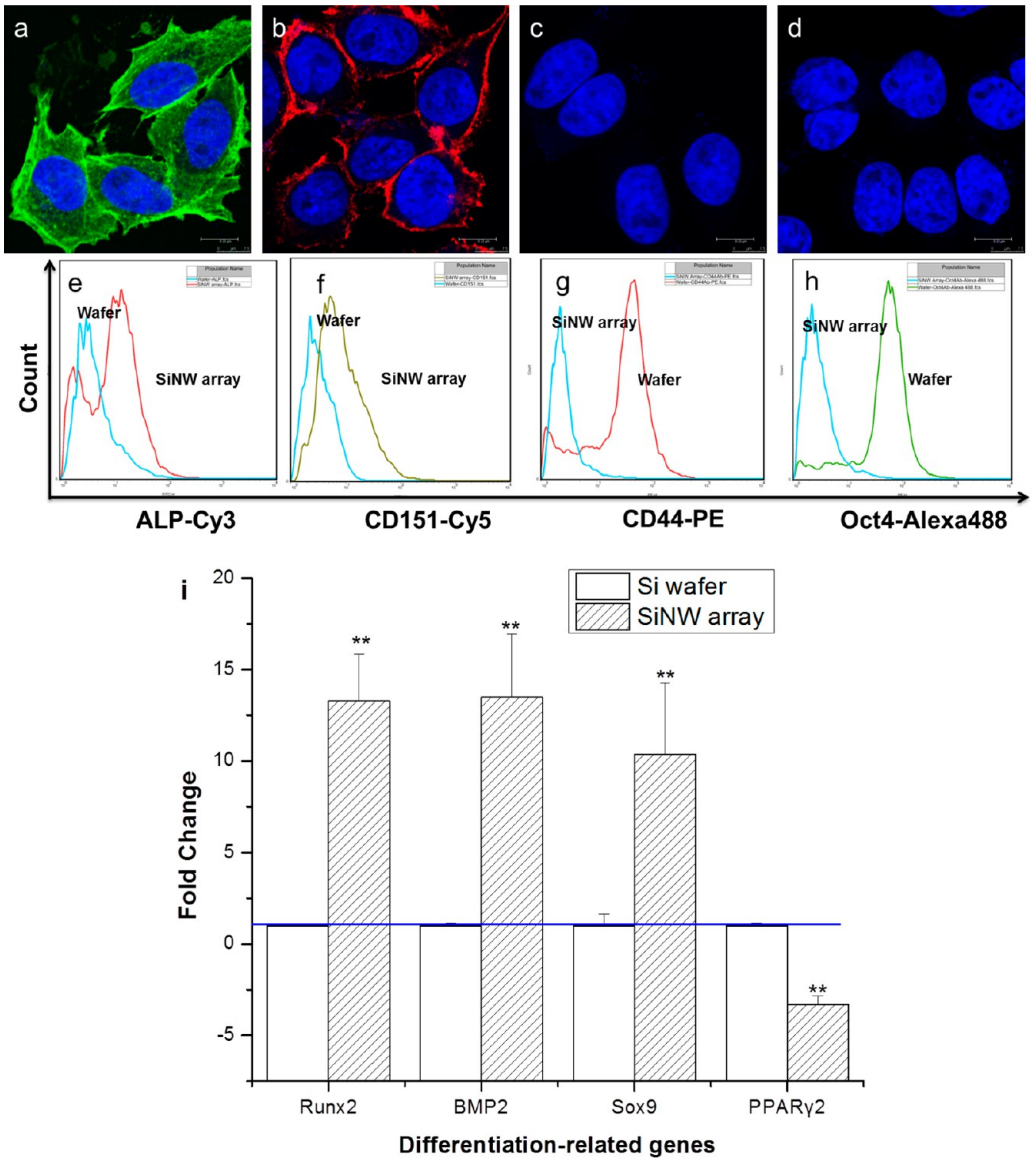

Figure 4. (a) Osteogenic and (b) chondrogenic differentiation of MSCs on SiNW arrays were confirmed by immunostaining with ALP-Cy3 and CD151-Cy5 antibodies, respectively; MSCs cultured on flat Si wafer showed negative immunostaining with ALP-Cy3 and CD151-Cy5 antibodies for (c) osteogenic and (d) chondrogenic differentiation, respectively. (e–h) Flow cytometry analysis of ALP, CD151, CD44, and Oct4 after MSCs incubated on wafer and SiNW array for 10 days, respectively. (i) Expression of genes related to osteogenesis, chondrogenesism, and adipogenesis as evaluated by qPCR. Data are representative of three separate trials. (*$P < 0.05$, **$P < 0.01$ vs wafer, $n = 5$).

extending from the cells and remained within the region where they were located. On the other hand, the morphology of MSCs attached on the flat Si wafer showed rounded shapes without filopodia or orientation and appeared to undergo apoptosis after 4 days of culture (Figure 3h and i). Flow cytometric analysis of MSCs cultured on the two different substrates further confirmed that less than 5% MSCs underwent apoptosis when cultured on the SiNW surface (Figure 3j), while more than 70% of MSCs were in the early apoptotic state after cultured on a flat Si wafer for 4 days (Figure 3k), as assessed by Annexin-V staining. The results further confirmed the enhanced adherent ability and viability of the MSCs on SiNW arrays.

3.4. Differentiation of MSCs on SiNW Arrays. Although much effort has been focused on the role of supplementary growth factors in MSC differentiation, little is known about the importance of mechanical stimuli in regulating MSC differentiation, particularly in the presence of nanomaterials.[27] In the present study, differentiation of MSCs in the microenvironment of SiNWs was assessed through the phenotypic staining and immunofluorescence staining of specific markers.

Although osteogenic and chondrogenic differentiation were on the same lineage direction of MSCs, they can be further distinguished by specific staining. ALP is a typical early marker for osteogenic differentiation, while CD151 was a characteristic marker for enhanced chondrogenesis potential.[28] The phenotype analysis (Figure 4a, b, e, and f) revealed that ALP and CD151 were expressed at significantly higher levels in MSCs cultured on SiNW arrays in the absence of supplementary growth factors. However, MSCs cultured on a flat Si wafer were negative for ALP and CD151 immunofluorescence staining (Figure 4c–f). The results suggested SiNW arrays prompted the capacity of MSCs toward osteogenic and chondrogenic differentiation. Meanwhile, MSCs cultured on the SiNW array

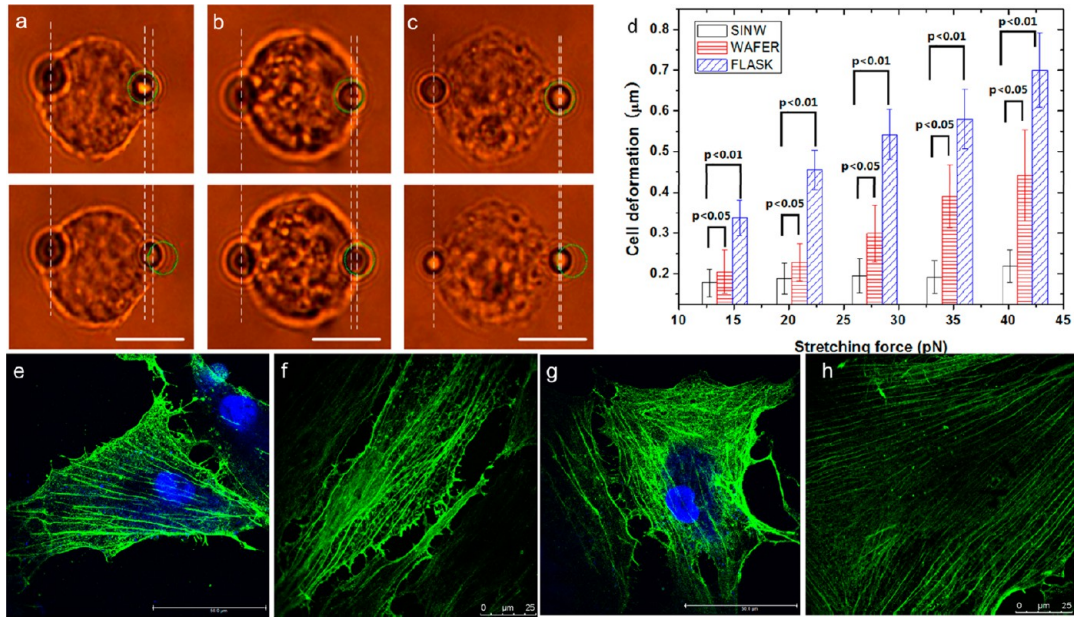

Figure 5. (a–c) Typical deformation response of MSCs cultured on (a) flask, (b) wafer, and (d) SiNW array. (d) Quantitative analysis of the mechanical responses of MSCs cultured on coverslip, wafer, and SiNW array. The error bar denotes the standard deviation of the results ($p < 0.05$ showed the significant difference). Cell images before (upper panel) and after stretching (lower panel). Scale bar = 10 μm. The green circle in the original image denotes the moving optical trap, while the patterns in the processed image denote the edges of the two beads. Confocal images of cytoskeleton organization in MSCs cultured on flat Si wafer (e and f) and SiNW array (g and h). In the confocal images, actins and nucleus were stained with antiactin antibody (green color) and DAPI (blue color), respectively.

seemed to gradually lose the stemness property as evaluated by the expression of CD44 and Oct4 (Figure 4g and h).

To further characterize the molecular response during the differentiation of MSCs, we determined the mRNA expression levels of several differentiation-related genes including bone morphogenetic protein 2 (BMP2), runt-related transcription factor 2 (Runx2), SRY-type HMG BOX transcription factor 9 (Sox9), and peroxisome proliferator-activated receptor-γ 2 (PPARγ2) (Figure 4i). BMP2 is involved in the early stages of bone formation and induces the expression of Runx2, which is principally linked to osteogenic differentiation.[29] As shown in Figure 4i, both BMP2 and Runx2 mRNA levels were significantly up-regulated in MSCs cultured on the SiNW array for 4 days without supplementary growth factors.

Sox9 is a member of the SRY-type HMG BOX transcription factor family and is required for promoting chondrogenesis and expressing type II collagen genes.[30] An increase in Sox9 mRNA level was observed in MSCs cultured on the SiNW array (Figure 4i), indicating the induction of chondrogenesis by the microenvironment of the SiNW array.

As adipogenic differentiation of MSCs is a reciprocal process of osteogenic differentiation, we further evaluated the expression of PPARγ2, which plays a central role in the control of adipogenesis of MSCs in a very early stage.[31] The results showed that the expression level of the PPARγ2 gene was down-regulated in MSCs after incubation on a SiNW array for 4 days (Figure 4i), suggesting that the SiNW array did not provide the niche for MSCs to undergo adipogenic differentiation. The transcriptional levels of the above genes appeared to be consistent with the phenotypic observation that SiNW arrays favored the differentiation of MSCs toward osteogenic and chondrogenic lineages.

3.5. Membrane Deformation and Cytoskeleton Organization in MSCs. The mechanical properties of cells, such as cytoskeleton organization and elasticity, membrane tension, cell shape, and adhesion strength, play a vital role in the regulation of MSC fate and differentiation.[32,33] Cell compliance is an important property, as the cells must undergo multiple deformations without compromising the structural integrity. Therefore, the mechanical properties of MSCs as reflected by the cell deformability and microfilament structures were measured by an optical tweezer technique and immunofluorescent staining technique, respectively, to evaluate the cytoskeleton organization during the differentiation process.

In the cell deformation experiments, MSCs cultured on different substrates for 7 days were stretched by an optical tweezer under the laser powers of 1, 1.5, 2, 2.5, and 3 W, respectively. The deformation and compliance of MSCs cultured on a flask (n = 33, Figure 5a), flat Si wafer (n = 29, Figure 5b), and SiNW (n = 35, Figure 5c) were determined, and the typical deformed images of MSCs under external stretching forces were shown in Figure 5a–c. The extents of cell deformation under the same conditions for MSCs cultured on different substrates in the absence of supplementary growth factors were summarized in Figure 5d. The results indicated that MSCs cultured on SiNW arrays were significantly stiffer than the control cells (cultured on flask) under the same stretching force ($p < 0.01$), they were also significantly stiffer than those cultured on a flat silicon wafer when the stretching force was larger than 34 pN ($p < 0.05$). These results indicated that the unique SiNW array microenvironment caused changes in the mechanical properties of MSCs through reorganization and deformation of cytoskeletons. The experimental results are consistent with the previous reports that Young's modulus of MSCs during differentiation is higher than the control group.[33,34]

The cytoskeletal reorganization of MSCs is a dynamic process depending on differentiated cell type, specification, morphogenesis stage, and environmental conditions. Actins are organized as thick bundles traversing the cell cytoplasm in

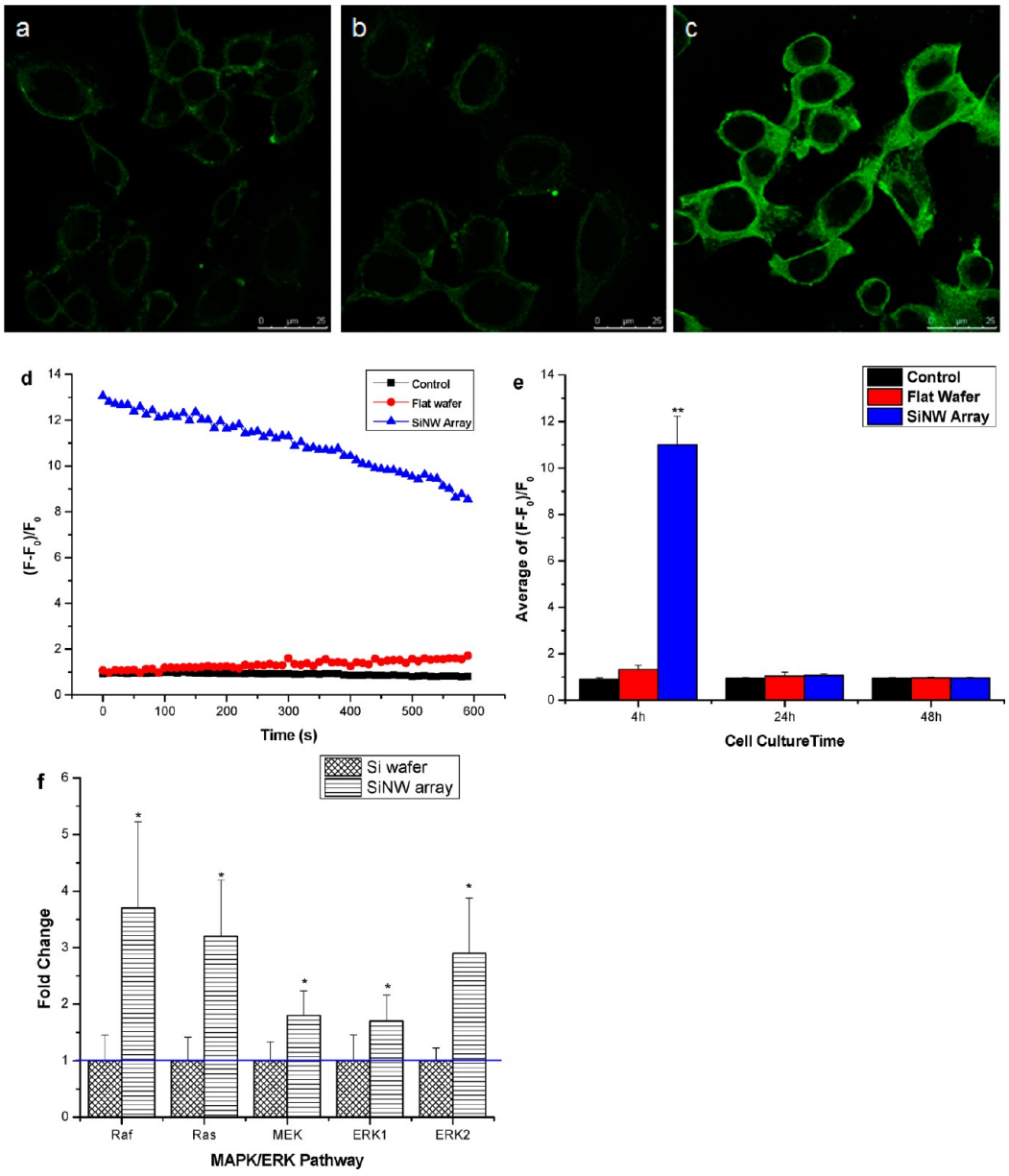

Figure 6. Fluorescence images of $[Ca^{2+}]_i$ in MSCs were captured using a fluorescent microscope with Fluo-3/AM when the cells were culuted on a coverslip (a), wafer (b), and SiNW array (c) for 4 h. (d) Quantification of cytosolic calcium concentrations. Cytosolic calcium was quantified by incubation with Fluo-3/AM in MSCs. (e) Averaged intracellular calcium concentration in MSCs after being cultured on different surfaces for 4, 24, and 48 h. (f) Expression of key genes involved in the MAPK/ERK pathway was evaluated by qPCR for MSCs cultred on a Si wafer and SiNW array for 4 h. Data are representative of three separate trials. (*$P < 0.05$, **$P < 0.01$ vs wafer, $n = 5$).

undifferentiated MSCs and as fine dense meshwork filling the cell interior in differentiated MSCs.[34,35] Consequently, plasma membrane binding to the cytoskeleton in MSCs constitutes an effective signaling pathway through membrane transport and ion channels by responding to the changing cytoskeleton. A significant difference between undifferentiated MSCs and differentiated MSCs in their cellular mechanics is their cytoskeleton organizations. The actin assemblies in MSCs cultured on Si wafer and MSCs cultured on SiNW arrays were shown in Figure 5e−h. MSCs cultured on flat Si wafer showed many thick bundles of actin filaments, or stress fibers, extending throughout the cytoplasm and terminating at focal contacts on the cell membrane. In contrast, MSCs cultured on a SiNW array demonstrated a thinner actin network with fewer stress fibers, indicating that MSCs have entered into differentiated states after being cultured on SiNW arrays for 7−14 days. The results from the above experiments indicated that for the MSCs cultured on the vertically aligned SiNW arrays, the changing morphology and adhesive behaviors may be associated with changes in the cytoskeleton structures to maintain the viability and adhesion ability.

3.6. Transient Activation of Ca^{2+} Ion Channels in MSCs Cultured on SiNW Arrays. We further investigated how MSCs sense changes in the microenvironment of the substrate and how external mechanical signals of the microenvironment are transmitted through the cytoskeleton to regulate cellular functions. One of the most important pathways to mediate mechanically regulated cell behaviors is the activation of the Ca^{2+} ion channels.[36] Mechanical stimulation can evoke cells to release mediators and intracellular calcium $[Ca^{2+}]_i$, which

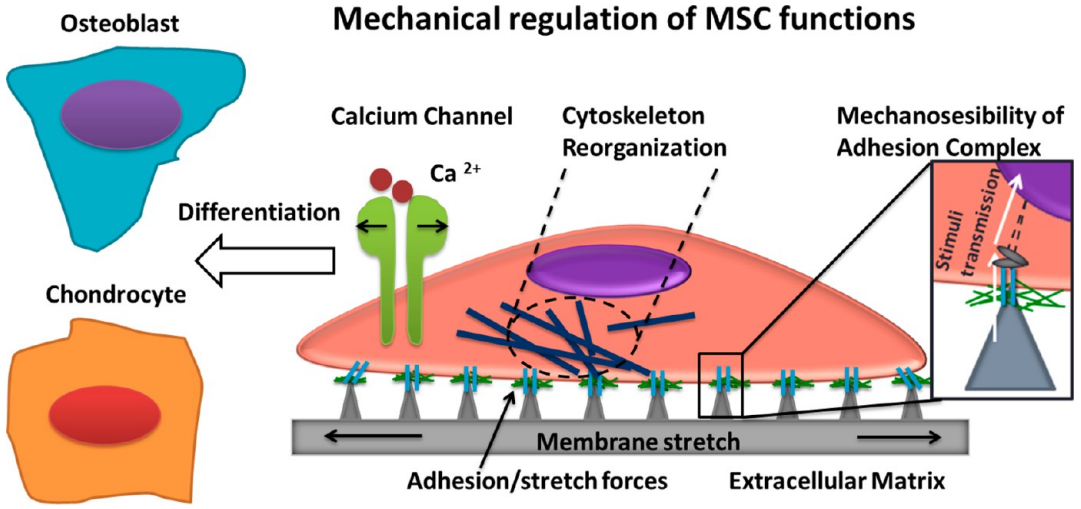

Figure 7. Schematic representation of stimuli transmission that regulates adhesion and differentiation of MSCs on the SiNW array.

influences the proliferation and differentiation of MSCs *in vivo* and *in vitro*.[37−39] Activation of Ca^{2+} ion channels results in a range of cellular responses including transcriptional regulation that ultimately lead to bone and cartilage matrix production. In this study, we hypothesized that Ca^{2+} ion channels were activated to serve as one of the specific mechanotransduction pathways during the early stage of MSC potentiation prior to differentiation. Our results showed that a transient increase in intracellular Ca^{2+} concentration ($[Ca^{2+}]_i$) occurred as one of the earliest responses of MSCs to a SiNW array microenvironment (Figure 6a−c). MSCs cultured on the control coverslip and flat Si wafer showed a basal $[Ca^{2+}]_i$ level (Figure 6d). When the MSCs were seeded on a SiNW array, $[Ca^{2+}]_i$ immediately increased and decreased steadily with time as MSCs adapted to the environment of the SiNW array (Figure 6d). The activation of Ca^{2+} channels in MSCs on SiNW arrays was only maintained during the first few hours of culturing (Figure 6e), indicating that Ca^{2+} ion channels were responsible for MSCs to sense the changing growth environment and initiate gene expression changes for the cells to adapt to the niche. It is well-known that incremental Ca^{2+} concentration modulated the Ras-dependent activation of the Ras/Raf/MEK/ERK signaling cascades, which regulate various aspects of cellular function, including the proliferation and differentiation of MSCs.[40] Indeed, significant up-regulation of the expressions of Ras, Raf, MEK, ERK1, and ERK2 (Figure 6f) after 4 h of culturing MSCs on SiNW arrays was observed, following the activation of the Ca^{2+} ion channels. The activation of the Ras/Raf/MEK/ERK signaling cascades eventually contributed to the up-regulation of genes related to osteogenesis and chandrogenesis and the down-regulation of genes related to adipogenesis (Figure 4i). Therefore, it is likely that the transient activation of Ca^{2+} ion channels during the initial and early stages of interaction between MSCs and the nanowire environment serves to transduce mechanosensitive signals from the extracellular matrix (ECM) into the cells upon external mechanical stimulation.

4. CONCLUSIONS

On the basis of the above results, a schematic diagram of how MSCs adhered to and interacted with the SiNW array was proposed (Figure 7). MSCs have the ability to sense and probe the mechanical properties of the surroundings and convert the mechanical stimuli into intracellular signaling cascades that ultimately influence cellular behaviors including adhesion, proliferation, and differentiation. The present study showed that the adhesion, proliferation, and differentiation of MSCs cultured on vertically aligned silicon nanowire (SiNW) arrays were significantly different from those on the flat silicon wafer and control substrates. The interactions between MSCs and the microenvironment of SiNW arrays caused the stem cells to preferentially differentiate toward osteocytes and chondrocytes but not adipocytes in the absence of supplementary growth factors. Our study demonstrated that the activation of Ca^{2+} ion channels appeared to be an early and transient event for MSCs upon mechanical stimulation, which eventually led to activation of Ras/Raf/MEK/ERK signaling cascades to regulate adhesion, proliferation, and differentiation of MSCs. Our results further revealed that stretch-mediated transient Ca^{2+} ion channel activation and cytoskeleton reorganization during the early stages of stem cell−nanowire interaction may serve as hallmarks of lineage-specific potentiation of MSCs in determining the fates of mesenchylmal stem cells when cultured in microenvironments with specific mechanical properties. Further study on the effects of SiNW density and surface modification on MSC differentiation and the detailed molecular pathways involved in the preferential differentiation of MSCs induced by SiNW arrays will enable us to understand the factors for precise control of chemical and/or mechanical stimulations, which will be critical for designing and developing novel scaffolds based on nanomaterials for tissue engineering and regenerative medicine.

AUTHOR INFORMATION

Corresponding Author

*E-mail: bhmyang@cityu.edu.hk.

Author Contributions

The manuscript was written through contributions of all authors. All authors have given approval to the final version of the manuscript.

Notes

The authors declare no competing financial interest.

ACKNOWLEDGMENTS

This work was supported by the Key Laboratory Funding Scheme of Shenzhen Municipal Government, China, the National Basic Research Program of China (973.

2012CB933302), and the General Research Fund of Hong Kong Research Grant Council, China (CityU_104411).

REFERENCES

(1) Langer, R.; Vacanti, J. P. *Science* **1993**, *260*, 920−926.
(2) Griffith, L. G.; Naughton, G. *Science* **2002**, *295*, 1009−1014.
(3) Liao, S.; Chan, C. K.; Ramakrishna, S. *Mater. Sci. Eng., C* **2008**, *28*, 1189−1202.
(4) Zhang, D.; Kilian, K. A. *Biomaterials* **2013**, *34*, 3962−3969.
(5) Tuan, R. S.; Boland, G.; Tuli, R. *Arthritis Res. Ther.* **2002**, *5*, 32−45.
(6) Thevenot, P.; Hu, W.; Tang, L. *Curr. Top. Med. Chem.* **2008**, *8*, 270−280.
(7) Dalby, M. J.; Gadegaard, N.; Tare, R.; Andar, A.; Riehle, M. O.; Herzyk, P.; Wilkinson, C. D.; Oreffo, R. O. *Nat. Mater.* **2007**, *6*, 997−1003.
(8) Nikukar, H.; Reid, S.; Tsimbouri, P. M.; Riehle, M. O.; Curtis, A. S. G.; Dalby, M. J. *ACS Nano* **2013**, *7*, 2758−2767.
(9) Shao, M. W.; Ma, D. D. D.; Lee, S. -T. *Eur. J. Inorg. Chem.* **2010**, *27*, 4264−4278.
(10) Peng, K. Q.; Lu, A. J.; Zhang, R. Q.; Lee, S. T. *Adv. Funct. Mater.* **2008**, *18*, 3026−3035.
(11) Alcaraz, J.; Buscemi, L.; Grabulosa, M.; Trepat, X.; Fabry, B.; Farré, R.; Navajas, D. *Biophys. J.* **2003**, *84*, 2071−2079.
(12) Matzke, R.; Jacobson, K.; Radmacher, M. *Nat. Cell Biol.* **2001**, *3*, 607−610.
(13) Bao, G.; Suresh, S. *Nat. Mater.* **2003**, *2*, 715−725.
(14) McBeath, R.; Pirone, D. M.; Nelson, C. M.; Bhadriraju, K.; Chen, C. S. *Dev. Cell* **2004**, *6*, 483−495.
(15) Faucheux, N.; Schweiss, R.; Lutzow, K.; Werner, C.; Groth, T. *Biomaterials* **2004**, *25*, 2721−2730.
(16) Zhang, B. H.; Wang, H. S.; Lu, L. H.; Ai, K.; Zhang, G.; Cheng, X. L. *Adv. Funct. Mater.* **2008**, *18*, 2348−2355.
(17) Liu, D. D.; Yi, D. C. Q.; Zhang, W.; Zhang, J. C.; Yang, M. S. *ACS Nano* **2010**, *4*, 2185−2195.
(18) Tan, Y. H.; Fung, T.-K.; Wan, H. X.; Wang, K. Q.; Leung, A. Y. H.; Sun, D. *Appl. Phys. Lett.* **2011**, *99*, 083702.
(19) Tan, Y. H.; Kong, C. W.; Chen, S.; Cheng, S. H.; Li, R. A.; Sun, D. *J. Biomech.* **2012**, *45*, 123−128.
(20) Wang, K. Q.; Sun, D. *J. Biomech.* **2012**, *45*, 1900−1908.
(21) Wang, Z. J.; Zhang, F. M.; Wang, L. S.; Yao, Y. W.; Zhao, Q.; Gao, X. *Cell Biol. Int.* **2009**, *33*, 665−674.
(22) Ladak, A.; Olson, J.; Tredget, E. E.; Gordon, T. *Exp. Neurol.* **2011**, *228*, 242−252.
(23) Wei, X.; Shen, C. Y. *Stem Cells Dev.* **2011**, *20*, 441−449.
(24) Balaban, N. Q.; Schwarz, U. S.; Riveline, D.; Goichberg, P.; Tzur, G.; Sabanay, I.; Mabalu, D.; Safran, S.; Bershadsky, A.; Addadi, L.; Geiger, B. *Nat. Cell Biol.* **2001**, *3*, 466−472.
(25) Kaufman, D. A.; Albelda, S. M.; Sun, J.; Davies, P. F. *Biochem. Biophys. Res. Commun.* **2004**, *320*, 1076−1081.
(26) Kim, W.; Ng, J. K.; Kunitake, M. E.; Conklin, B. R.; Yang, P. D. *J. Am. Chem. Soc.* **2007**, *129*, 7228−7229.
(27) Ainslie, K. M.; Bachelder, E. M.; Borkar, S.; Zahr, A. S.; Sen, A.; Badding, J. V.; Pishko, M. V. *Langmuir* **2007**, *23*, 747−754.
(28) Adesida, A. B.; Mulet-Sierra, A.; Jomha, N. *Curr. Stem Cell Res. Ther.* **2012**, *3*, 9−21.
(29) Gersbach, C. A.; Guldberg, R. E.; Garcia, A. J. *J. Cell. Biochem.* **2007**, *100*, 1324−1336.
(30) Martinez-Sanchez, A.; Dudek, K. A.; Murphy, C. L. *J. Biol. Chem.* **2012**, *287*, 916−924.
(31) Takahashi, A.; Morita, M.; Yokoyama, K.; Suzuki, T.; Yamamoto, T. *Mol. Cell. Biol.* **2012**, *32*, 5067−5077.
(32) Settleman, J. *Mol. Cell* **2004**, *14*, 148−150.
(33) Titushkin, I.; Cho, M. *Biophys. J.* **2007**, *93*, 3693−3702.
(34) Rodriguez, J. P.; Gonzalez, M.; Rios, S.; Cambiazo, V. *J. Cell. Biochem.* **2004**, *93*, 721−731.
(35) Yu, H. Y.; Tay, C. Y.; Leong, W. S.; Tan, S. C. W.; Liao, K.; Tan, L. P. *Biochem. Biophys. Res. Commun.* **2010**, *393*, 150−155.
(36) Dreses-Werringloer, U.; Vingtdeux, V.; Zhao, H.; Chandakkar, P.; Davies, P.; Marambaud, P. *J. Cell Sci.* **2013**, *126*, 1199−1206.
(37) Tuan, R. S.; Boland, G.; Tuli, R. *Arthritis Res. Ther.* **2003**, *5*, 32−45.
(38) Jaffe, L. F. *Biol. Cell* **2007**, *99*, 175−184.
(39) Felix, J. A.; Chaban, V. V.; Woodruff, M. L.; Dirksen, E. R. *Am. J. Respir. Cell Mol. Biol.* **1998**, *18*, 602−610.
(40) Cullen, P. J.; Lockyer, P. J. *Nat. Rev. Mol. Cell Biol.* **2002**, *3*, 339−348.